ISSN 1674-1056
http://cpb.iphy.ac.cn
http://iopscience.iop.org/cpb
中国物理 B
Chinese Physics
中国物理 Chinese Physics B

Heavy fermions in high magnetic fields

M Smidman, B Shen(沈斌), C Y Guo(郭春煜), L Jiao(焦琳), X Lu(路欣), H Q Yuan(袁辉球)

Citation: Chin. Phys. B . 2019, 28(1): 017106. **doi:** 10.1088/1674-1056/28/1/017106
Journal homepage: http://cpb.iphy.ac.cn; http://iopscience.iop.org/cpb

What follows is a list of articles you may be interested in

Pressure effect in the Kondo semimetal $CeRu_4Sn_6$ with nontrivial topology

Jiahao Zhang(张佳浩), Shuai Zhang(张帅), Ziheng Chen(陈子珩), Meng Lv(吕孟), Hengcan Zhao(赵恒灿), Yi-feng Yang(杨义峰), Genfu Chen(陈根富), Peijie Sun(孙培杰)

Chin. Phys. B . 2018, 27(9): 097103. **doi:** 10.1088/1674-1056/27/9/097103

Voltage-controlled Kosterlitz-Thouless transitions and various kinds of Kondo behaviors in a triple dot device

Yong-Chen Xiong(熊永臣), Jun Zhang(张俊), Wang-Huai Zhou(周望怀), Amel Laref

Chin. Phys. B . 2017, 26(9): 097102. **doi:** 10.1088/1674-1056/26/9/097102

Anisotropic and mutable magnetization in Kondo lattice $CeSb_2$

Yun Zhang(张云), Xiegang Zhu(朱燮刚), Bingfeng Hu(胡丙锋), Shiyong Tan(谭世勇), Donghua Xie(谢东华), Wei Feng(冯卫), Qin Liu(刘琴), Wen Zhang(张文), Yu Liu(刘瑜), Haifeng Song(宋海峰), Lizhu Luo(罗丽珠), Zhengjun Zhang(张政军), Xinchun Lai(赖新春)

Chin. Phys. B . 2017, 26(6): 067102. **doi:** 10.1088/1674-1056/26/6/067102

Electronic structure and magnetic properties of rare-earth perovskite gallates from first principles

A Dahani, H Alamri, B Merabet, A Zaoui, S Kacimi, A Boukortt, M Bejar

Chin. Phys. B . 2017, 26(1): 017101. **doi:** 10.1088/1674-1056/26/1/017101

Hybrid density functional study on lattice vibration, thermodynamic properties, and chemical bonding of plutonium monocarbide

Rong Yang(杨荣), Bin Tang(唐斌), Tao Gao(高涛), Bing-Yun Ao(敖冰云)

Chin. Phys. B . 2016, 25(6): 067106. **doi:** 10.1088/1674-1056/25/6/067106

TOPICAL REVIEW — Fundamental research under high magnetic fields

Heavy fermions in high magnetic fields*

M Smidman[1], B Shen(沈斌)[1], C Y Guo(郭春煜)[1], L Jiao(焦琳)[1], X Lu(路欣)[1,2], and H Q Yuan(袁辉球)[1,2,†]

[1] Center for Correlated Matter and Department of Physics, Zhejiang University, Hangzhou 310058, China
[2] Collaborative Innovation Center of Advanced Microstructures, Nanjing University, Nanjing 210093, China

(Received 6 November 2018; published online 27 December 2018)

Heavy fermion materials are prototypical strongly correlated electron systems, where the strong electron–electron interactions lead to a wide range of novel phenomena and emergent phases of matter. Due to the low energy scales, the relative strengths of the Ruderman–Kittel–Kasuya–Yosida (RKKY) and Kondo interactions can often be readily tuned by non-thermal control parameters such as pressure, doping, or applied magnetic fields, which can give rise to quantum criticality and unconventional superconductivity. Here we provide a brief overview of research into heavy fermion materials in high magnetic fields, focussing on three main areas. Firstly we review the use of magnetic fields as a tuning parameter, and in particular the ability to realize different varieties of quantum critical behaviors. We then discuss the properties of heavy fermion superconductors in magnetic fields, where experiments in applied fields can reveal the nature of the order parameter, and induce new novel phenomena. Finally we report recent studies of topological Kondo systems, including topological Kondo insulators and Kondo–Weyl semimetals. Here experiments in magnetic fields can be used to probe the topologically non-trivial Fermi surface, as well as related field-induced phenomena such as the chiral anomaly and topological Hall effect.

Keywords: heavy fermions, high magnetic fields, quantum phase transitions, heavy fermion superconductivity, topological Kondo systems

PACS: 71.27.+a, 74.70.–b, 74.70.Tx **DOI:** 10.1088/1674-1056/28/1/017106

1. Introduction

Heavy fermion compounds are canonical examples of systems in which there are strong electron–electron correlations. These are intermetallic compounds containing certain rare earth atoms with unpaired f-electrons, typically Ce, Pr, Yb, U, etc. While in the isolated case, the f-electron shell is localized to the atoms, in heavy fermion materials there is hybridization between the f-electrons and the conduction electrons via the Kondo interaction.[1] This favors the formation of a Kondo singlet at low temperatures, where the f-electron spin is screened by the conduction electrons.

In heavy fermion materials, the effects of a single f-electron cannot be considered alone, but the arrangement of atoms into a lattice must be taken into account.[1,2] In these systems, two competing interactions need to be considered, the Ruderman–Kittel–Kasuya–Yosida (RKKY) interaction which leads to the ordering of f-electron moments,[3–5] and the Kondo interaction which leads to a non-magnetic ground state. In the Doniach model, the relative strengths of these interactions are tuned by the same coupling constant J, leading to magnetic order for weak coupling.[6] As J is increased, the Kondo interaction eventually gets stronger more rapidly than the RKKY interaction, leading to the suppression of the magnetic order. The ordering temperature can often be reduced to zero at a quantum critical point, where quantum rather than thermal fluctuations drive the properties, leading to unusual phenomena such as non-Fermi liquid behavior, unconventional superconductivity, or other novel phases. The energy scales of heavy fermion systems are generally low and therefore many materials can be tuned through the Doniach phase diagram using various non-thermal parameters such as pressure, doping, or applied magnetic fields.[7,8]

Experiments in high magnetic fields have been very important for understanding the behavior of heavy fermion systems, for instance:

(i) Field as a tuning parameter. Along with pressure and doping, magnetic fields have been used to tune heavy fermion systems. In general, a sufficiently large magnetic field will destroy the Kondo effect, breaking up the Kondo singlets. However, there are examples where field can tune the system to suppress magnetic order, leading to quantum critical behavior. One notable example is $YbRh_2Si_2$, where the field-induced quantum critical point is believed to be an unconventional local type at which the Kondo effect is destroyed.[9,10]

(ii) Probing quantum criticality via Fermi surface measurements. One of the notable effects of the Kondo effect in heavy fermion systems is that at low temperatures there is often a reconstruction of the Fermi surface, where the electronic bands pick up a very large effective mass. An important ex-

*Project supported by the National Natural Science Foundation of China (Grant No. U1632275), the National Key R&D Program of China (Grant Nos. 2017YFA0303100 and 2016YFA0300202), and the Science Challenge Project of China (Grant No. TZ2016004).

†Corresponding author. E-mail: hqyuan@zju.edu.cn

© 2019 Chinese Physical Society and IOP Publishing Ltd

perimental method for probing the Fermi surface is via the de-Haas van-Alphen effect, where the periodicity of the quantum oscillations corresponds to the extremal cross sectional areas of the Fermi surface, and their temperature dependence gives the effective quasiparticle mass. For heavy fermion systems, a consequence of the greatly enhanced effective quasiparticle masses is that characterizing the Fermi surface requires much larger magnetic fields, as well as lower temperatures. There is particular interest in looking at how the Fermi surface is affected as a function of tuning parameters such as field or pressure. It has been proposed that quantum critical points can be classified as either conventional spin density wave (SDW) types or unconventional local types depending on how the Fermi surface changes crossing the quantum critical point at zero temperature.[11–13] At a local quantum critical point, the Kondo effect breaks down and therefore there is a sudden change from a large Fermi surface involving the f-electrons to a small Fermi surface where the f-electrons are fully localized.

(iii) Topological heavy fermion systems. Topological condensed matter systems have been much studied after the discovery that the electronic structures of many materials can be classified as topologically non-trivial. In the case of topological insulators, this implies that even if there is insulating behavior in the bulk, the surface must conduct. The material SmB_6 has attracted considerable attention, since it has been proposed to be a topological Kondo insulator, where the gap in the topological band structure opens due to the hybridization between the conduction and f electrons.[14] Measurements in field have been very important for probing the fascinating properties. For instance, despite the apparent bulk insulating state, quantum oscillations have been observed in SmB_6 and there has been considerable debate over whether these originate from the conducting surface states[15] or if they are a bulk property.[16,17] Furthermore, field-based thermodynamic and transport measurements have been useful to confirm the presence of conducting surface states,[18–20] as well as to exclude the presence of bulk excitations.[21] Meanwhile heavy fermion systems with gapless topological states have also become of particular interest recently, specifically those which may host Dirac or Weyl points, where there is a linear band crossing with excitations which can be described as Dirac or Weyl fermions.[23,24] High field measurements are vital for studying topological correlated systems. In particular, quantum oscillations are an important tool for revealing the band topology, where an analysis of the field dependence of the Landau indices can reveal whether there is a non-trivial Berry phase.[24–27] Furthermore, systems with Dirac or Weyl fermions exhibit unusual magnetotransport properties, where a negative magnetoresistance when the field and current are parallel is a signature of the chiral anomaly in Weyl fermion systems.[28–32]

2. Quantum critical points tuned by multiple parameters

2.1. Introduction to quantum critical Ce-based heavy fermions

Heavy fermion materials can often be tuned by various parameters such as pressure, doping, or magnetic fields. A schematic phase diagram for Ce-based heavy fermion systems under pressure is displayed in Fig. 1(a),[33] based on the temperature–pressure phase diagram of $CeCu_2(Si_{1-x}Ge_x)_2$ displayed in Fig. 1(b).[34] The application of pressure first suppresses magnetic order to a quantum critical point (labelled p_{c1}), and the system enters a heavy fermion state. In this region, there is a dome of superconductivity mediated by spin fluctuations. This superconductivity is suppressed as pressure further increases the hybridization, but at higher pressures still, there is a second dome of superconductivity in the region of p_{c2}, well away from magnetic order. It has been proposed that the superconductivity in this second dome is mediated by valence fluctuations,[33–35] suggesting that the system is in close proximity to a valence transition.

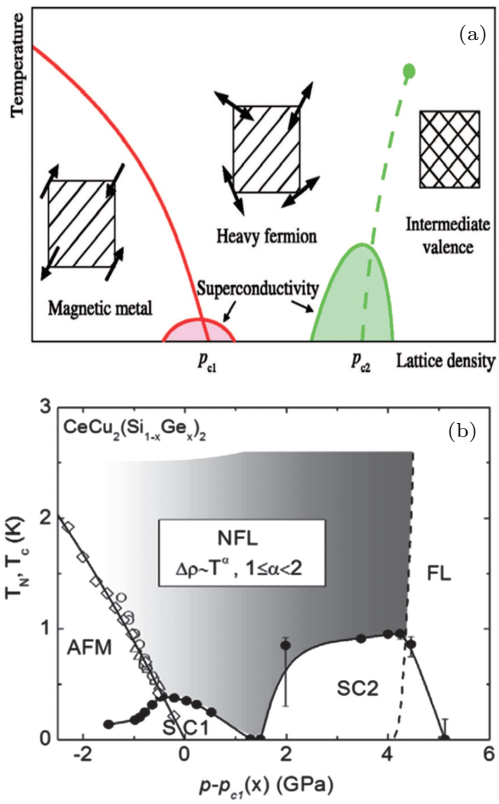


Fig. 1. (a) A schematic temperature–pressure phase diagram for Ce-based heavy fermion systems under pressure. Reprinted from Yuan *et al.*, Ref. [33]. Copyright 2003 AAAS. (b) Temperature–pressure phase diagram of $CeCu_2(Si_{1-x}Ge_x)_2$ reproduced with permission from Yuan *et al.*, Ref. [34]. Copyright 2006 by the American Physical Society.

One of the richest sources of novel physics in heavy fermion compounds has been the $Ce_nT_mIn_{3n+2m}$ (T = transition metal) series of compounds. $CeIn_3$ is a cubic compound which orders antiferromagnetically at $T_N = 10.2$ K.[36]

The magnetic order is suppressed by applying pressure and T_N reaches zero at a critical pressure of around $p_c = 2.6$ GPa. In this region of the phase diagram, there is a dome of superconductivity with a maximum T_c less than 0.3 K.[37] Following on from this, the CeTIn$_5$ (T = Co, Ir, or Rh) family of compounds were discovered, where layers of CeIn$_3$ are interspersed with TIn$_2$, leading to an overall much more two-dimensional layered structure.[38–40] At ambient pressure, both CeCoIn$_5$ and CeIrIn$_5$ are superconductors with respective bulk T_c values of 2.2 K and 0.4 K, while CeRhIn$_5$ is an antiferromagnet with $T_N = 3.8$ K. The temperature–pressure phase diagram of CeRhIn$_5$ is displayed in Fig. 2.[41,42] Upon applying pressure, T_N is suppressed and a superconducting dome emerges. The superconductivity and antiferromagnetism coexist up until $p* = 1.75$ GPa, where T_N and the superconducting T_c are equal. At higher pressures, T_N is not observed, but measurements in-field reveal the reemergence of magnetism and a quantum critical point at $p_c = 2.3$ GPa.[42]

Meanwhile the Ce$_2T$In$_8$ (T = Co, Pd or Rh) series are another structural variant which also show either superconductivity at ambient pressure or antiferromagnetism with pressure induced superconductivity.[43–45]

As a result, the Ce$_n T_m$In$_{3n+2m}$ families of compounds have been very important for studying heavy fermion behavior, magnetism, superconductivity, and the interplay between all of these phenomena. Furthermore, measurements under high applied magnetic fields have been vital for understanding many of the properties displayed in these materials. Below we give an overview of some of the results elucidated from such measurements under field.

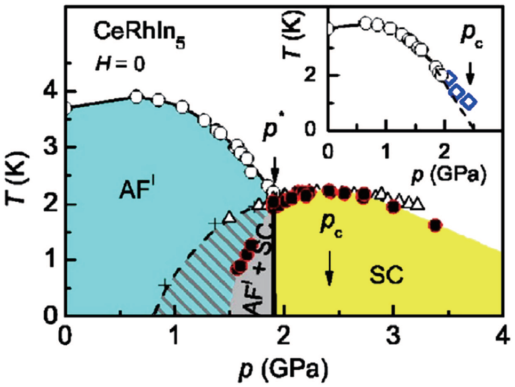


Fig. 2. Temperature–pressure phase diagram of CeRhIn$_5$ reproduced with permission from Knebel *et al.*, Ref. [41]. Copyright 2006 by the American Physical Society. The antiferromagnetism (AF) is suppressed by pressure until $p*$ where the AF dome meets the superconducting (SC) dome. The quantum critical point p_c lies at higher pressure within the SC dome.

2.2. Fermi surface studies of CeTIn$_5$

A particular interest for studies of the CeTIn$_5$ materials has been to uncover how the Fermi surface evolves as the various interactions are tuned. CeRhIn$_5$ is different from both CeCoIn$_5$ and CeIrIn$_5$ in that at ambient pressure there is antiferromagnetic order, which indicates the dominance of the RKKY interaction and a weaker Kondo effect in CeRhIn$_5$. This is consistent with studies of the Fermi surface which show that the 4f electrons are well localized in CeRhIn$_5$, but in CeCoIn$_5$ and CeIrIn$_5$ they are itinerant and contribute to the Fermi surface.[46–48] It is therefore said that CeRhIn$_5$ has a small Fermi surface, while the other two materials have large Fermi surfaces. It was found that in CeRhIn$_5$ at the quantum critical point $p_c = 2.3$ GPa, where antiferromagnetism is suppressed (Fig. 2), there is a sharp change of the dHvA frequencies and a dramatic increase of the effective quasiparticle mass.[49] These new frequencies were found to be in good agreement with those of CeCoIn$_5$, suggesting that at the pressure induced quantum critical point there is a sudden Fermi surface reconstruction from a small Fermi surface to a large Fermi surface. This may correspond to the scenario of a local quantum critical point where there is a breakdown of the Kondo effect at p_c, below which the Kondo singlet does not fully form at the lowest temperatures.[11–13]

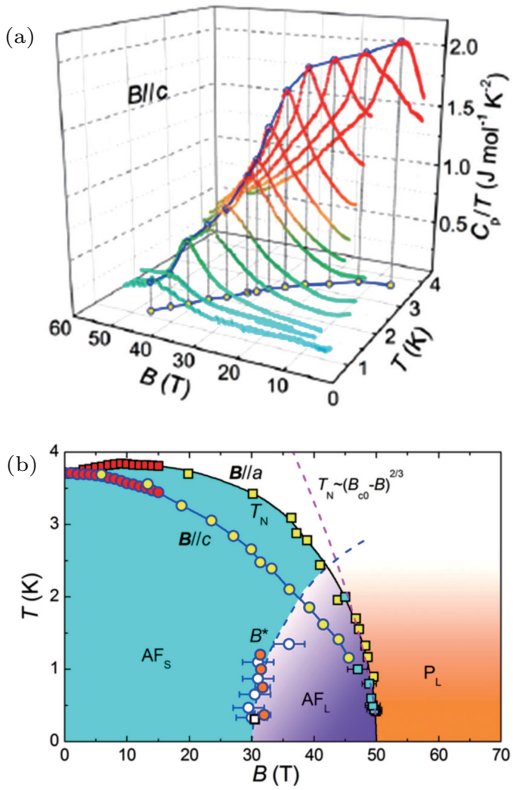


Fig. 3. (a) Magnetic field dependence of the heat capacity of CeRhIn$_5$ at various temperatures when the field is along the c-axis. (b) Field–temperature phase diagram of CeRhIn$_5$ for fields along the a- and c-axes. AF and P denote antiferromagnetism and paramagnetism, respectively, while the subscripts mark a small (S) or large (L) Fermi surface. Reproduced from Jiao *et al.*, Ref. [48].

It was therefore desirable to measure the effects of tuning CeRhIn$_5$ using high magnetic fields. This allows for a comparison between the uses of pressure and field as tuning parameters, and the robustness of the magnetism to applied field

allows the change of Fermi surface as a function of field to be probed in the magnetic state.

The temperature–field phase diagram is displayed in Fig. 3 from Ref. [48], for fields applied along both the a-axis and c-axis. At lower fields, there is a significant anisotropy in the critical fields for the two field directions, as anticipated for a very two-dimensional layered structure. However, at higher fields the two critical field curves converge and the magnetic transition is suppressed to zero temperature at a field induced quantum critical point at $B_{c0} = 50$ T. The more three-dimensional nature of the system at higher fields is reflected in the observation of $T_N \propto (B_{c0} - B)^{2/3}$, which is the expected behavior for three-dimensional spin fluctuations.

Moreover, a clear reconstruction of the Fermi surface is found upon increasing the field, but in this instance it occurs well below the quantum critical point at $B^* = 30$ T, deep inside the antiferromagnetic state. This is clearly illustrated in Fig. 4 for measurements using a piezo-cantilever up to 45 T. The upper inset of Fig. 4(a) shows the oscillations after subtracting the background, where there is a clear change around B^* with much more rapid oscillations. To examine the field dependence of the Fermi surface, fast Fourier transforms were performed on the dHvA data over different field windows. As shown in Fig. 4(b), a number of new frequencies emerge at high fields above B^*, where the frequencies have much larger values. A more detailed comparison is displayed in Fig. 5 from Ref. [51]. At low fields below B^*, it can clearly be seen that the dHvA frequencies of $CeRhIn_5$ and $LaRhIn_5$ are very similar, again indicating that they have very similar Fermi surfaces. Since $LaRhIn_5$ does not have any f-electrons, this is consistent with previous reports that at low fields, the f-electrons of $CeRhIn_5$ are well localized. However as displayed in Fig. 5(c), the new frequencies above B^* are quite close to those of $CeCoIn_5$, where the f-electrons are itinerant and contribute to the Fermi surface. This analysis indicates that at B^* there is a reconstruction of the Fermi surface from a small Fermi surface at low fields to a large Fermi surface at higher fields, where the f-electrons become delocalized. This scenario is further supported by high field Hall resistivity measurements shown in Fig. 6. Upon reducing the temperature, two clear features emerge in the Hall coefficient as a function of field applied parallel to the c-axis. There is an anomaly observed at a field below B^*, which is denoted by B_M and likely ascribed to a metamagnetic transition. Meanwhile at B^* there is a dramatic drop of the Hall coefficient, which gets more pronounced at lower temperatures and this corresponds to a sudden change of carrier density, indicative of a Fermi surface reconstruction at B^*. Following this discovery, a pronounced anisotropy of the in-plane resistivity was found to occur above B^*,[52] which was ascribed to a spin nematic phase, indicating that this change of electronic structure is accompanied by the emergence of novel phases of matter.

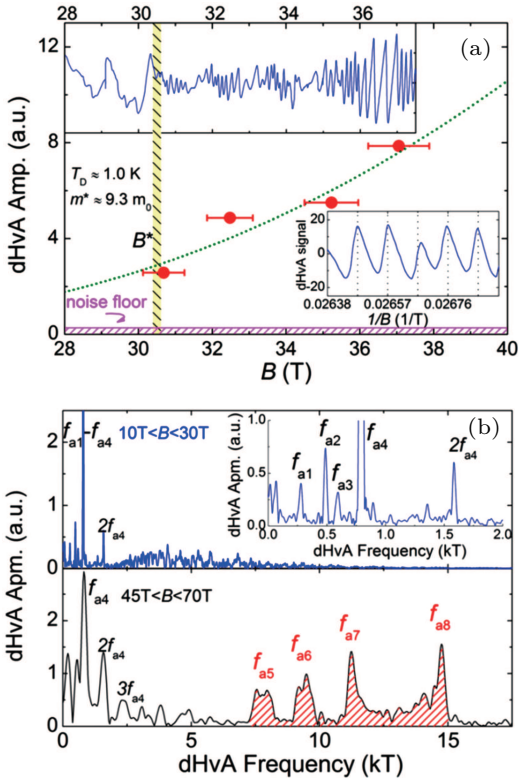


Fig. 4. (a) dHvA measurements of $CeRhIn_5$ at high fields parallel to the a-axis performed using a piezo-cantilever in a hybrid magnet up to 45 T. The main panel shows the field dependence of the dHvA amplitude of one of the new frequencies above B^*. The inset at the top shows the oscillations after subtracting the background while the $1/B$ dependence is shown in the lower inset. (b) The Fourier transforms of the dHvA data for a field window below (10 T$< B <$ 30 T) and above (45 T$< B <$ 70 T) B^*. Both reproduced from from Jiao *et al.*, Ref. [48].

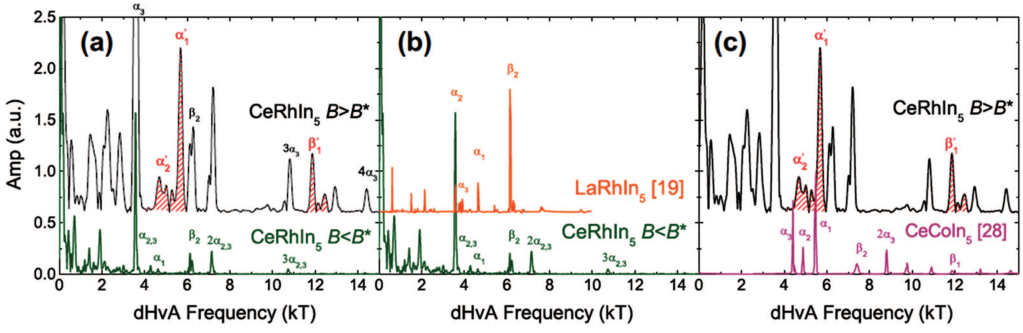


Fig. 5. A comparison between the fast Fourier transforms of the dHvA spectra of (a) $CeRhIn_5$ at $B > B^*$ and $B < B^*$, (b) $CeRhIn_5$ at $B < B^*$ and $LaRhIn_5$ from Ref. [41], and (c) $CeRhIn_5$ at $B > B^*$ and $CeCoIn_5$ from Ref. [50]. All reproduced from Jiao *et al.*, Ref. [51].

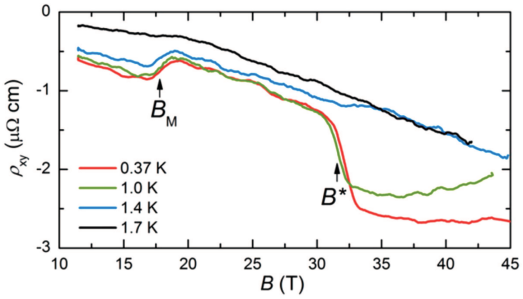


Fig. 6. The Hall coefficient of $CeRhIn_5$ as a function of field applied parallel to the *c*-axis, reproduced from Jiao *et al.*, Ref. [48].

The observation of a field induced reconstruction of the Fermi surface within the antiferromagnetic state is markedly different to that when pressure is applied, where the Fermi surface reconstruction occurs at the quantum critical point. This indicates that the field induced quantum critical point is of the conventional SDW-type, while the pressure induced quantum critical point is the unconventional local type. The possibility of two different types of QCP found from tuning the same material with two different parameters needs to be explored further, in particular to find whether QCPs can be universally classified.

2.3. Field-induced quantum critical point in Ce_2PdIn_8

Compared to the $CeTIn_5$ materials, the Ce_2TIn_8 family has been much less frequently studied, but the presence of superconductivity in two members at ambient pressure makes them an interesting topic for study. Ce_2PdIn_8 is one of these materials, displaying superconductivity at $T_c = 0.68$ K.[45] A further interesting feature is that an applied magnetic field is a good tuning parameter, and evidence was found for a field induced quantum critical point.[53] At zero-field, a superconducting transition is observed in resistivity measurements, which is suppressed as a field is applied.

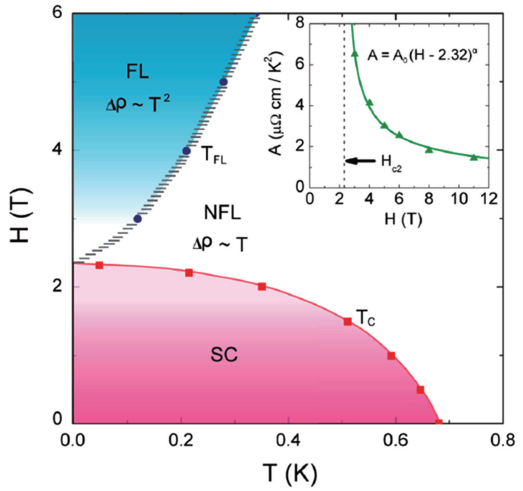


Fig. 7. Field–temperature phase diagram of Ce_2PdIn_8 obtained from resistivity measurements. The superconducting (SC), non-Fermi liquid (NFL), and Fermi liquid (FL) regions are all labeled. Figure reproduced from Dong *et al.*, Ref. [53].

For fields greater than around 2.4 T, no superconducting transition is found down to 50 mK and the temperature dependence of the resistivity is linear. This indicates the presence of non-Fermi liquid behavior, instead of the $\sim T^2$ dependence of Fermi liquid theory. Meanwhile, at higher fields, the Fermi liquid behavior is again observed and the temperature below which the $\sim T^2$ dependence is found (T_{FL}) increases with increasing field, as displayed in the phase diagram in Fig. 7. It is also found that the coefficient of the $\sim T^2$ behavior (A) sharply increases approaching the upper critical field. All these results give evidence for the presence of a field-induced quantum critical point coinciding with the suppression of superconductivity at the upper critical field of Ce_2PdIn_8. Similar behavior was suggested to occur in $CeCoIn_5$,[54,55] pointing to a degree of universality between the nature of these two families of materials.

2.4. Field-tuning in frustrated magnetic system CePdAl

One particularly promising avenue for exploring the multiple types of QCP is to look for highly frustrated heavy fermion systems, since this has been proposed to promote the unconventional local QCP scenario.[11–13] In a frustrated system, all contributions to the potential energy cannot be simultaneously minimized and two basic effects that introduce frustration to a system are lattice geometric frustration[56] and frustration due to irreconcilable exchange interactions.[57] For example, frustration in magnetic systems arises when the spin configurations cannot be optimized to minimize all the spin interaction energies. In a general heavy fermion phase diagram, besides tuning the hybridization strength between localized moments and the conduction electrons, frustration can add another dimension to the phase diagram that drives the system into intriguing emergent states, as illustrated in Fig. 8.[58–60] Magnetic fields can tune a system in this two-dimensional phase diagram, but the exact role that an external magnetic field plays needs more theoretical studies and experimental investigations.

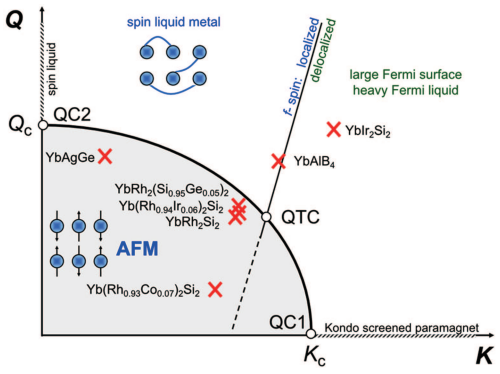


Fig. 8. Generic global phase diagram displaying the combined effects of Kondo coupling (K) and magnetic frustration, or quantum zero-point motion (Q), reproduced with permission from Custers *et al.*, Ref. [60]. Copyright 2010 by the American Physical Society.

A good candidate for studying frustration is the heavy fermion compound CePdAl with a distorted Kagome lattice.[61] By fitting six inequivalent nuclear Bragg peaks and thirteen inequivalent magnetic Bragg peaks obtained by powder neutron diffraction,[62] it was concluded that CePdAl is a partially frustrated system in which only two thirds of the Ce moments form long-range antiferromagnetic order with a Neel temperature $T_N = 2.7$ K, while the other one third of the Ce moments are disordered due to geometric frustration. This magnetic structure is in agreement with a group theoretical analysis.[62]

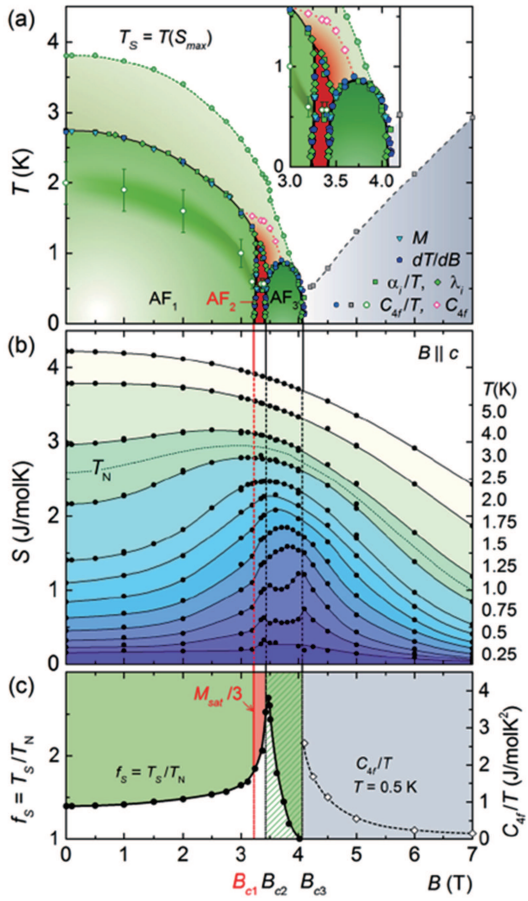


Fig. 9. Magnetic phase diagram of CePdAl for $B \parallel c$ obtained from measurements of different properties. The subscript i for α_i and λ_i denotes the different axes a or c. Open circles indicate the approximate temperature of the broad shoulders of C_{4f}/T below T_N, gray squares the position of the maxima of the Schottky anomalies, and red open diamonds the temperature of the C_{4f} maximum. The inset shows an enlarged view of the AF_2 and AF_3 phases. (b) Entropy $S(B)$ at different fixed temperatures. (c) Frustration parameter $f_S = T_S/T_N$ vs. B. For $B > B_{c3}$, C_{4f}/T at $T = 0.5$ K is plotted against B. All lines are guides to the eye. Figure reproduced with permission from Lucas *et al.*, Ref. [64]. Copyright 2017 by the American Physical Society.

For the heavy fermion compound CePdAl, the frustrated moments are screened leading to a heavy fermion state at low temperatures and the intersite correlations between the frustrated moments are likely to be removed, which is supported by neutron scattering[62] and NMR[63] measurements. Upon applying a magnetic field, the Neel temperature is smoothly suppressed initially but goes through several metamagnetic transitions to AF_2 and AF_3 phases, in the field range of 3.2–4.0 T as shown in Fig. 9.[64] A detailed resistivity and susceptibility study on CePdAl by Sun's group[65] also shows a similar magnetic field phase diagram, however, crossover behavior is reported to exist between the AF_3 and high field phases shown by the grey shading.

The hybridization strength can be tuned by field and it is possible to liberate the frustrated moments from Kondo screening prior to the suppression of AFM, yielding a metallic spin liquid state in a certain field range. A comprehensive entropy analysis of CePdAl as a function of field[64] suggests that the frustration level is enhanced when crossing the phase boundary at $B_{c1} \sim 3.25$ T and reaches its highest value at $B_{c2} \sim 3.4$ T from AF_2 to AF_3 phase, confirming the boosted frustration and entropy as shown in Fig. 9. It is interpreted that the liberated Ce moments interact with the ordered AF moments and destabilize the AFM order at B_{c1}. In the AF_3 phase, the unstable frustrated state yields a different magnetic ground state with a lifting of the frustration above $B_{c3} \sim 4.1$ T. These results strongly suggest that the AF_2 phase in CePdAl is a promising candidate for a metallic spin liquid phase. However, further careful studies are necessary to address this possibility.

3. In-field superconducting properties of heavy fermion superconductors

3.1. Superconducting order parameters of CeTIn$_5$

Characterizing the order parameter symmetry of the superconducting state is important for understanding the nature of the superconductivity and the microscopic mechanism leading to its formation and an important aspect of this is measuring the structure of the superconducting gap. In the case of the CeTIn$_5$ materials, the presence of line nodes, that is lines across the Fermi surface where the superconducting gap goes to zero, could be inferred in $CeCoIn_5$ and $CeIrIn_5$ from zero-field measurements of the specific heat,[66] thermal conductivity,[66] and magnetic penetration depth.[67,68] However measurements in field allow for not only the presence of nodes to be ascertained but for their positions in $\boldsymbol{k}$ space to be probed.

In Fig. 10, the heat capacity of $CeIrIn_5$ at 2.05 GPa is displayed from Ref. [69] for fields applied at an azimuthal angle ϕ to the [100] direction. The heat capacity shows a clear fourfold oscillation upon rotating the field through 360°. Besides measurements at the highest field, all the measurements show a minimum along the [100] direction and a maximum along [110]. Although in a simple classical picture this would imply line nodes along [100], this only applies at very low temperatures and fields,[70] and in fact the results suggest line nodes

along [110]. This 45° shift of the positions of the minima and maxima is observed in $CeCoIn_5$ upon increasing the temperature in an applied field of 1 T.[71] These results allow for the pairing state to be narrowed further, since although there are several unconventional pairing states with line nodes, only the $d_{x^2-y^2}$ state has four-fold symmetry with nodes along [110] and therefore field dependent heat capacity and thermal conductivity measurements indicate the presence of a $d_{x^2-y^2}$ state in $CeCoIn_5$ and $CeIrIn_5$.[71–73]

3.2. Intertwined order parameters and the *Q*-phase in $CeCoIn_5$

Applied magnetic fields can also lead to additional novel behaviors in superconductors. The application of magnetic fields generally leads to the breaking of Cooper pairs by two mechanisms, the orbital effect and paramagnetic limiting. The orbital pair breaking effect arises from the kinetic energy of supercurrents surrounding the vortex flux lines making the superconducting state energetically unfavorable. Meanwhile the paramagnetic limiting effect arises from the Zeeman splitting of the electron bands. When this Zeeman energy becomes sufficiently large compared to the superconducting condensation energy, superconductivity will often be destroyed. Although in most superconducting systems the orbital limiting effect primarily determines the magnitude of the upper critical field, when the paramagnetic limiting mechanism dominates, novel phases have been predicted such as the Fulde–Ferrell–Larkin–Ovchinnikov (FFLO) state.[74,75] This state has a spatially modulated order parameter including a periodic arrangement of normal and superconducting regions, and the Cooper pairs have a finite center-of-mass momentum.

$CeCoIn_5$ had been considered to be a good candidate for the realization of the FFLO state, which has the required dominance of paramagnetic limiting and is in the clean limit.[66,76] Furthermore it was found that at fields larger than 4.7 T applied along the *c*-axis (temperatures below $0.31T_c$), the transition from the normal to superconducting state changes from second-order to first-order, which is expected for Pauli limited superconductors.[76] In addition, at higher fields in the region where the superconducting to normal transition is first-order, an additional transition was found in specific heat measurements at lower temperatures in the superconducting state,[77,78] which was taken as evidence for the FFLO state. In particular, it was found that this transition at T_{FFLO} disappeared when $T_c < T_{FFLO}$, demonstrating an intrinsic link between this transition and the superconducting phase. Meanwhile, while NMR studies all found distinct changes in this high field '*Q*'-phase, conflicting results were also reported.[79–81] In one study, the appearance of a new higher field resonance line was reported within the *Q*-phase, where the value of the Knight shift rapidly approached the normal state value with decreasing temperature.[79] This was taken as evidence for the coexistence of normal and superconducting regions in this high field regime, and therefore indicated that this did indeed correspond to the FFLO phase. On the other hand, different results were reported in another NMR study, where it was found that the spin-susceptibility in the *Q*-phase was enhanced compared to that in the homogenous superconducting state, yet still less than the normal state value.[80] This is inconsistent with the simple picture of alternating normal and superconducting regions in the FFLO state. It was also subsequently reported that the broadening of the NMR spectra was different for each of the crystallographic sites.[81] Such a variation cannot be simply explained by the inhomogeneity arising from the modulation of the order parameter in the FFLO state, since the length scales of these variations are considerably larger than the unit cell, and therefore it would be expected that there should be no difference for the different sites. Instead, these results give evidence for the occurrence of long range magnetic order of localized Ce moments. These

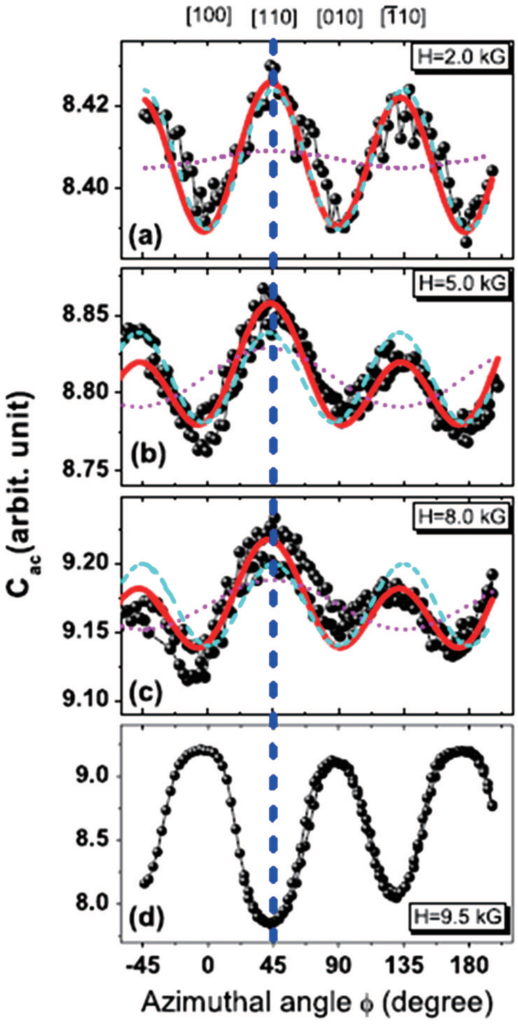


Fig. 10. Field-angle dependence of the heat capacity of $CeIrIn_5$ at 2.05 GPa, when a field is applied at an angle ϕ to the [100] direction. Figure reproduced with permission from Lu *et al.*, Ref. [69]. Copyright 2002 by the American Physical Society.

unusual results point to a very different relationship between superconducting and magnetism in $CeCoIn_5$, where instead of an antagonistic relationship between these phases, the occurrence of superconductivity is required for the appearance of long range magnetic order.

Direct evidence for this magnetic order was later reported in single crystal neutron diffraction measurements for fields applied along the [1-10] direction, where magnetic Bragg peaks corresponding to an ordering wavevector of (q, q, 0.5) were reported, with $q \sim 0.44$ (Fig. 11).[82] This magnetic structure has an incommensurate modulation within the *ab*-plane but is commensurate along the *c*-axis, and has a small ordered moment of around 0.15 μ_B/Ce aligned along the *c*-axis. The peak width was limited by the resolution of the instrument, showing that the correlation length of the magnetic order exceeded 60 nm, which is significantly larger than the vortex cores, thereby showing that the magnetism is not purely constrained to the core region. Importantly, the incommensurate modulation q is nearly field independent, and therefore inconsistent with the simple picture of the FFLO state, where the wave-vector of the real space modulation of the order parameter is expected to be proportional to the applied field. Further important findings were revealed by neutron scattering measurements along the [100] direction.[83] Here a very similar ordering wave vector was found of (q, q, 0.5) with $q \sim 0.45$, and therefore contrary to the assumptions of many theoretical proposals at the time, the ordering wave vector is constrained to lie along the nodal directions of the $d_{x^2-y^2}$ order parameter, instead of rotating to be aligned with the field.

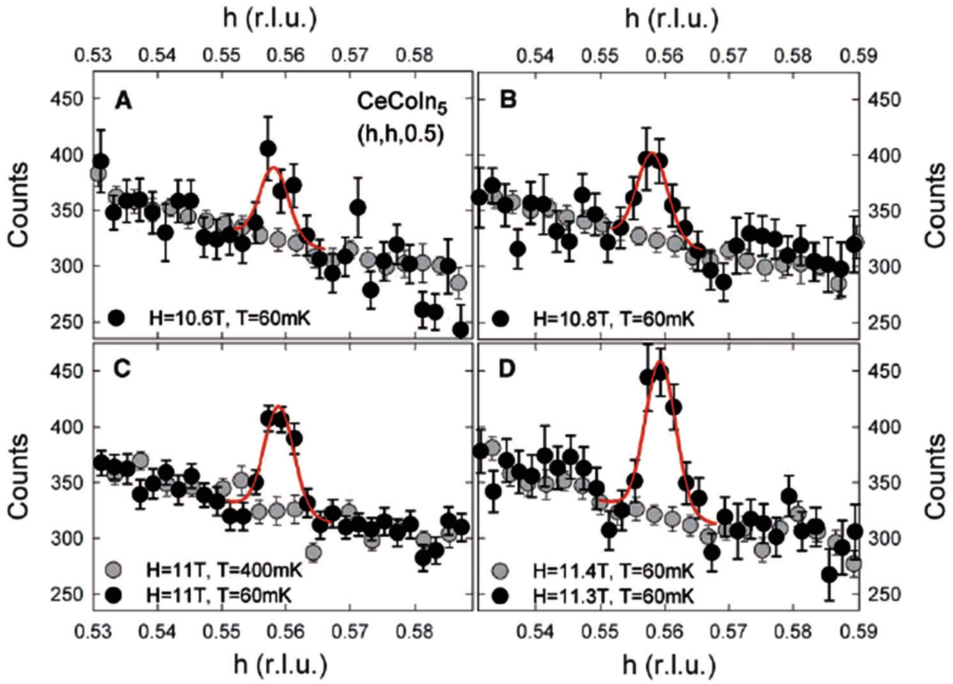


Fig. 11. Neutron diffraction intensity at a position (h, h, 0.5) as a function of h for $CeCoIn_5$ measured in various high fields close to H_{c2}. The black circles display the data in the superconducting state, while the grey circles are in the normal state. It can be seen that in the superconducting state the magnetic Bragg peak appears corresponding to the *Q*-phase, which is absent when the system becomes normal. Figure reproduced with permission from Kenzelmann *et al.*, Ref. [82]. Copyright 2008 AAAS.

In general, for a magnetic ordering wave vector (q, q, 0.5), there are two possible SDW domains, one with $\boldsymbol{Q}_h = (q, q, 0.5)$ and the other with $\boldsymbol{Q}_v = (q, -q, 0.5)$. Remarkably, it was found from neutron diffraction measurements in the *Q*-phase with a field rotated in the *ab*-plane that only one of these domains is found to occur (Fig. 12).[84] That is when a field is applied along the [1-11] direction, only the SDW domains with an ordering wave-vector perpendicular to the field direction $\boldsymbol{Q}_h$ are populated. Meanwhile as the field is rotated away from [1-10] again only the peaks corresponding to $\boldsymbol{Q}_h$ are observed, until the field is rotated beyond [100] where there is an abrupt change, and only the $\boldsymbol{Q}_v$ domains are populated (Fig. 12). Therefore there is always a single domain structure, even for fields along [100] when both domains should be equivalent. These highly unusual results were explained by theoretical proposals based on the presence of a spatially modulated p-wave pair density wave state, which was proposed to occur from the coupling between d-wave superconductivity and SDW phases.[85,86] Here the additional p-wave order parameter has a pair of lobes separated by a line node. For a field along [1-10], the lobes of the p-wave order parameter align with the field, gapping the d-wave line node in the field direction, but leaving a nodal direction along [110]. Consequently, only the SDW domains with $\boldsymbol{Q}$ along the nodal direction ($\boldsymbol{Q}_h$) are allowed to occur. Meanwhile the flipping of the direction of the p-wave order parameter in turn leads to a flipping of the

populated SDW domain. Further evidence for this scenario was found from thermal conductivity measurements.[87] Here distinct differences were seen for measurements when the heat current was parallel and perpendicular to the direction of the ordering vector of the populated domain. Furthermore these results could not be explained simply by the opening of a gap parallel to the SDW wave-vector, since they pointed to a larger gap being opened in the direction perpendicular to that of the populated SDW domain. This is therefore consistent with the pair density wave scenario, where the p-wave order parameter opens a gap along one of the nodal directions of the d-wave order parameter. This state with both d-wave superconductivity and a triplet pair density wave state has a modulation in real space, which arises due to the intricate connection between the superconducting and magnetic orders.[84]

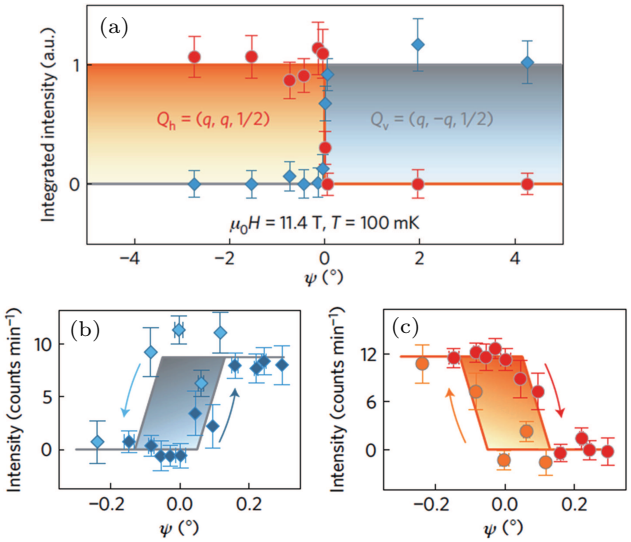


Fig. 12. (a) The intensity of the neutron diffraction peaks of the two SDW vectors $\boldsymbol{Q}_h = (q, q, 0.5)$ and $\boldsymbol{Q}_v = (q, -q, 0.5)$ as a function of the direction of the applied 11.4 T field in the vicinity of the [100] direction. Here the angle ϕ corresponds to the angle relative to [100]. It can be seen that upon tilting the field beyond [100], there is an abrupt depopulation of one SDW domain and complete population of the other. (b), (c) The hysteresis of this abrupt switch of the domains about the [100] direction, confirming that this is a first order process. All figures are reproduced with permission from Macmillan Publishers Ltd: Nature Physics (Ref. [84]), copyright 2014.

4. Correlated topological systems in high magnetic fields

4.1. Topological Kondo insulator SmB_6 with anomalous quantum oscillations

In intermetallic systems, the observation of quantum oscillations in high magnetic fields provides important information about the Fermi surface, while in insulators, the lack of electronic bands crossing the Fermi level should preclude the occurrence of quantum oscillations. However, this seemingly obvious truth was called into question following the discovery of quantum oscillations in the Kondo insulator SmB_6 via high field measurements of the dHvA effect.[15–17]

Two aspects in particular appear to separate SmB_6 from regular band insulators. Firstly, SmB_6 has generally been considered to be a Kondo insulator where the insulating gap opens at low temperatures due to the strong electronic correlations. As a result of the strong hybridization between the lattice of 4f electrons and the conduction electrons, renormalized heavy bands with very large effective masses form at low temperatures, separated by a hybridization gap. In Kondo insulators, the Fermi level lies within this gap, yielding a low temperature insulating state.[88] In SmB_6, this is manifested by an extremely large increase in the resistivity at low temperatures, which increases as the temperature is decreased.[89,90] More recently, it was proposed that some Kondo insulators can also be characterized as topological insulators.[14] In this case, the resulting insulating electronic structure emerging due to the strong hybridization has a non-trivial Z_2 index. Here the bulk band structure corresponds to a different topological index to the vacuum, which has a trivial topology. As a result, at the boundary between the bulk and vacuum, i.e., the surface of the sample, the insulating gap must vanish, and therefore conducting metallic surface states are anticipated. One of the longstanding mysteries of SmB_6 is that below around 4 K, rather than continuing to decrease with decreasing temperature, the resistivity plateaus and changes little as the material is further cooled. Recent careful transport measurements have suggested that these "in-gap" states in fact correspond to surface conduction, providing experimental evidence for conducting surface states and therefore for SmB_6 being a topological Kondo insulator.[18–20,91–93]

Besides the anomalous low temperature conduction, another unusual observation for an insulator found in SmB_6 is that of quantum oscillations via measurements of the dHvA effect. This phenomenon has been reported by two different research groups using torque magnetometry, on samples grown by two different methods, as displayed in Fig. 13.[15,16] However, the two different studies came to strikingly different conclusions about the origins of these oscillations. In the case of Li *et al.*,[15] the oscillation frequencies were reported to increase strikingly upon rotating the field by 45°, as displayed in Fig. 14. This was taken as a clear indication of the two-dimensionality of the Fermi surface, which is evidence that the quantum oscillations arise from the metallic surface states, rather than the insulating bulk.

On the other hand, Tan *et al.*[16] also observed quantum oscillations, which were reported over a wider frequency range, up to values larger than $10k_BT$. It was suggested by the authors that such large frequencies cannot be accounted for by surface states, due to the need for a correspondingly large mean-free path longer than the depth of the surface layers. Moreover, the angular dependences of the frequencies, which are also displayed in Fig. 14, were reported to be much more

three-dimensional, and hence were ascribed to the bulk of the sample. It was also suggested that the Fermi surface is rather similar to other rare-earth hexaborides such as LaB_6, CeB_6, and PrB_6. It was pointed out that due to the robustness of the insulating gap of SmB_6 up to high fields of at least 45 T, this cannot be accounted for by quantum oscillations from a gapless high field state. Consequently, the origin of the quantum oscillations in SmB_6 are hotly contested, and a number of theoretical proposals have been made based on both surface[94] and bulk[95,96] origins for this unusual phenomenon.

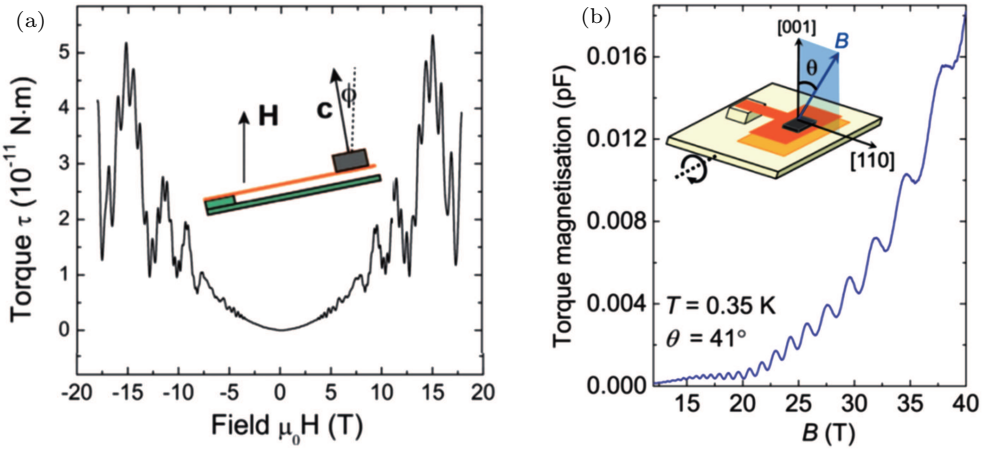


Fig. 13. Quantum oscillations in the topological Kondo insulator SmB_6 from measurements of the field dependence of the torque magnetometry. The measurements were performed by two different groups, with panel (a) reprinted with permission from Li *et al.*, Ref. [15]; copyright 2014 AAAS, and panel (b) reprinted with permission from Tan *et al.*, Ref. [16]; copyright 2015 AAAS.

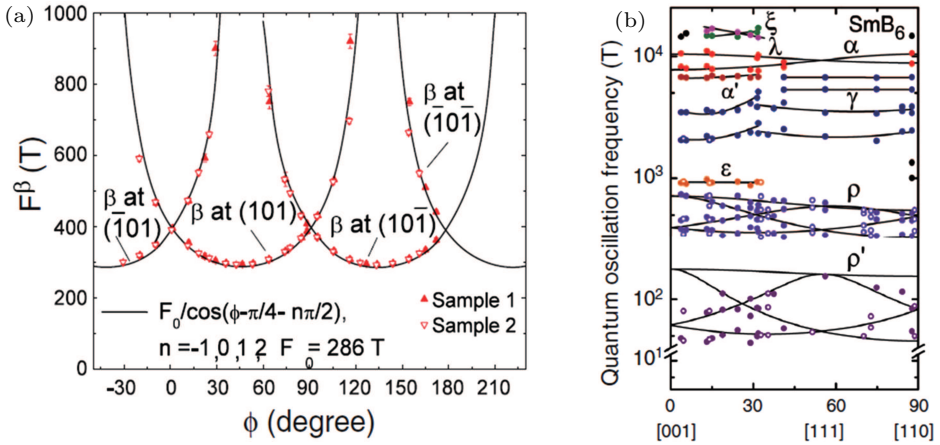


Fig. 14. Angular dependence of the quantum oscillation frequencies of SmB_6 from Ref. [15] (a) and Ref. [16] (b). In the case of the former, the angular dependence was reported as being consistent with a 2D Fermi surface, as expected if the quantum oscillations arise from a surface state. On the other hand, the angular dependence of the frequencies in panel (b) was reported to be much more consistent with three-dimensional Fermi surfaces, pointing to a bulk origin. Panel (a) is reprinted with permission from Li *et al.*, Ref. [15]; copyright 2014 AAAS, and panel (b) is reprinted with permission from Tan *et al.*, Ref. [16]; copyright 2015 AAAS.

4.2. High field studies of correlated semimetals

Topological Kondo insulators are examples of gapped topological materials, where there is a gap in the topologically non-trivial bulk electronic structure, and the Fermi level lies within the gap. Recently, gapless topological semimetals with strong electronic correlations have also been increasingly studied. Examples of gapless topological materials include Dirac and Weyl semimetals, which have bulk band structures hosting linear band crossings, where the nearby excitations are well described by either Dirac or Weyl fermions, respectively.[22,23,97–100] It is of particular interest then to explore examples of such topological materials with strong electronic correlations, to examine the interplay of these two effects.

The R(Sb,Bi) (R = rare earth) family of materials are examples where these effects have been studied, in particular due to the potential for tuning the correlations and electronic structure by substituting with different rare earth elements. Studies of this series of materials were spurred by the finding that LaSb shows a plateau in the resistivity at low temperatures, which was suggested to be similar to that seen in SmB_6,[101] although angle resolved photoemission spectroscopy (ARPES) studies cannot agree whether there is a non-trivial topology.[102,103]

High field measurements have been important for probing the non-trivial topology in these materials in two principal ways. Firstly, studies of quantum oscillations either using the dHvA or SdH effects can be utilized to probe the non-trivial

Fermi surface, in particular they can be used to look for a non-trivial Berry phase. This can be performed by analyzing the Landau indices, whereby the oscillations are examined as a function of $1/B$, the positions of either the oscillation maxima or minima are indexed, and the data are fitted linearly to determine the residual value. Here the value of the residual Landau index provides information about whether or not there is a non-trivial Berry phase, as well as the dimensionality of the Fermi surface.[24,25] For these measurements, high magnetic fields are particularly important, so as to probe the low lying Landau indices, allowing for an accurate determination of the intercept. The analysis of SdH oscillations in SmSb revealed a residual Landau index corresponding to a non-trivial Berry phase, which could be determined with a low degree of uncertainty due to magnetoresistance measurements being performed in pulsed fields up to 60 T.[27] Moreover, at low temperatures there was a significant deviation in the temperature dependence of the SdH oscillation amplitudes which could not be accounted for by the Lifshitz–Kosevich expression. A deviation from Lifshitz–Kosevich theory has also been observed in some dHvA measurements of SmB_6,[16] but in the case of SmSb, anomalous behavior is only seen in SdH oscillations, whereas dHvA measurements show standard behavior. On the other hand, other *R*Sb compounds such as PrSb show evidence for a trivial Berry phase from the Landau index analysis,[104] suggesting that substituting for different rare earth elements can tune the band topology.[105,106]

Another important probe for looking for Weyl fermions is from the presence of the chiral anomaly, which can be inferred from a negative longitudinal magnetoresistance. Weyl semimetals host Weyl points with different chiralities, and the chiral anomaly arises due to the parallel magnetic and electric fields pumping charges from one Weyl point to another of opposite chirality, which in turn leads to a population imbalance.[28,29] Evidence for Weyl fermions was found in the magnetic Kondo system CeSb from the observation of signatures of the chiral anomaly from the measurements of the longitudinal magnetoresistance. CeSb orders antiferromagnetically at low temperatures, but as shown in Fig. 15(a), in the field-induced ferromagnetic state a negative longitudinal magnetoresistance is observed, where a slight rotation of the field away from the current direction destroys this effect.[31] This scenario is accounted for by electronic structure calculations, which show that in zero-field there is a non-trivial band structure with band inversions.[31] In the field-induced ferromagnetic state, the Zeeman field splits the degeneracy of the bands, except at non-trivial band crossing points corresponding to Weyl nodes, which is illustrated in Fig. 15(b).

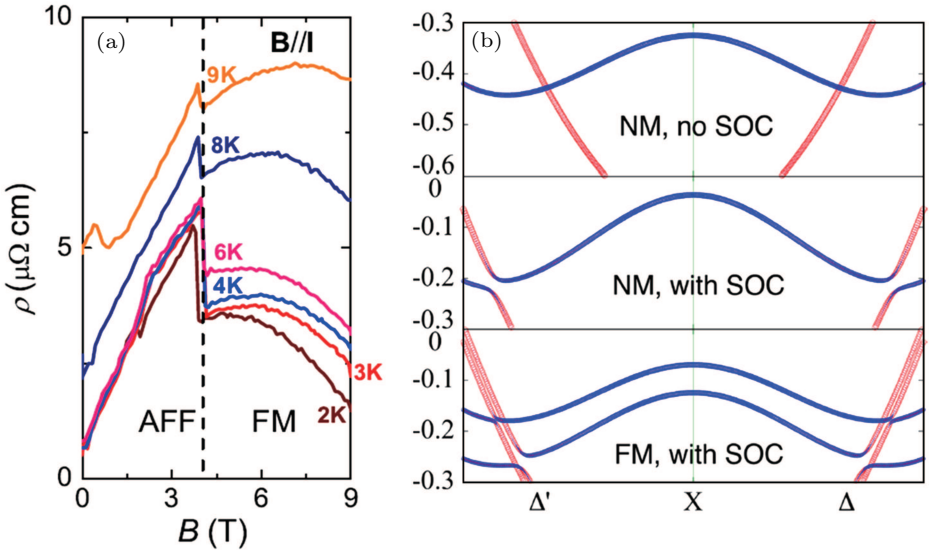


Fig. 15. (a) Resistivity of CeSb as a function of field, when the applied field is parallel to the current direction. At low temperatures, a negative longitudinal magnetoresistance is observed after the transition from the antiferro-ferromagnetic (AFF) state to the field-induced ferromagnetic (FM) state. (b) Schematic diagram of how Weyl nodes occur in the field induced FM state of CeSb. The spin–orbit coupling gaps out the degenerate band crossing points, giving rise to a band inversion. The breaking of time reversal symmetry in the field-induced FM state splits the degenerate bands, giving rise to doubly degenerate band crossing points, which correspond to Weyl nodes. Both panels are reproduced from Guo *et al.*, Ref. [31].

Meanwhile evidence for Weyl fermions from magnetotransport measurements was also observed in the heavy fermion semimetal YbPtBi,[32] where the extremely large Sommerfeld coefficient of around 8 $J{\cdot}mol^{-1}{\cdot}K^{-2}$ indicates that the electronic bands are strongly renormalized at low temperatures due to the Kondo interaction.[107] At elevated temperatures above 20 K, the magnetotransport shows clear signatures of the chiral anomaly, exhibiting the expected temperature, field, field-angle, and doping dependences.[32] Furthermore, the presence of Weyl fermions is supported by the electronic structure calculations and ARPES measurements, showing evidence for triply degenerate fermion points in zero field, which are each split into a Weyl point and a trivial crossing in applied fields. At low temperatures, the evidence for the

chiral anomaly disappears, yet as displayed in Fig. 16, evidence for Weyl fermions is found from a pronounced topological Hall effect, as well as a T^3 dependence of the specific heat, which can be accounted for by the strong renormalization of the electronic bands dramatically reducing the Fermi velocity v^*. This evolution of the Weyl points as the charge carriers pick up a large effective mass at low temperatures, is illustrated in Fig. 17,[32] where the greatly reduced v^* due to the Kondo effect leads to a negligible chiral anomaly contribution to the conductivity c_a, but a sizeable specific heat term $C_e/T^3 \sim (1/v^*)^3$. As such, YbPtBi offers the prospect of studying the interplay of topology, strong correlations, and quantum criticality.

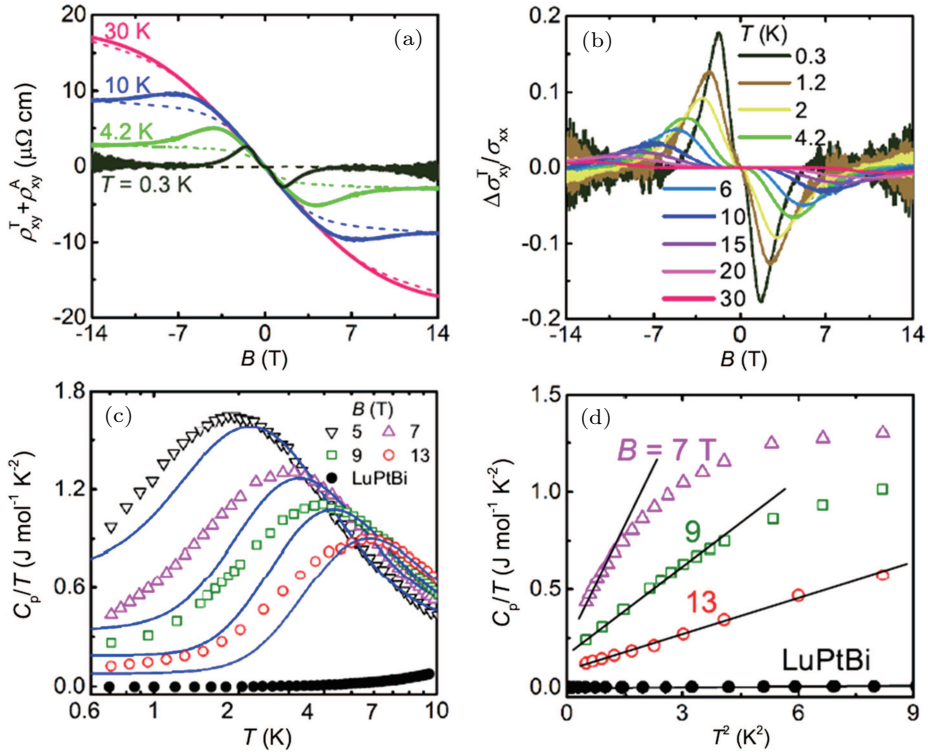


Fig. 16. Evidence for Weyl fermions at low temperatures in the heavy fermion state of YbPtBi. (a) Anomalous contribution to the Hall resistivity, after subtracting the normal contribution from the charge carriers. (b) Topological Hall angle at different temperatures after subtracting a contribution from the Hall resistivity proportional to the magnetization. The significant value at low temperatures arises from the Berry curvature generated by the Weyl nodes. (c) Temperature dependence of the specific heat as C_p/T in various applied fields. The solid line shows a fit to a Kondo model, which cannot describe the low temperature data. (d) C_p/T vs. T^2 in various applied fields. The linear relationship reveals a cubic temperature dependence of the specific heat, which is a signature of the linear dispersion of heavy fermion bands expected in the vicinity of Weyl points. Figure reproduced from Guo *et al.*, Ref. [32].

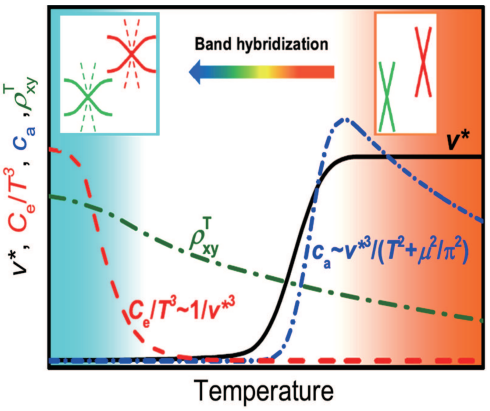


Fig. 17. Schematic diagram to illustrate the evolution of Weyl fermions in YbPtBi, as the temperature is reduced and the Kondo interaction becomes stronger. The dramatic decrease of the Fermi velocity v^* at low temperatures leads to the disappearance of the chiral anomaly contribution c_a, but the large entropy associated with the renormalized bands leads to a sizeable cubic term in the temperature dependence of the specific heat C_e. Meanwhile a sizeable topological Hall effect contribution ρ_{xy}^T can be detected in both the low and intermediate temperature ranges, arising from the Berry curvature generated by the Weyl points. Figure reproduced from Guo *et al.*, Ref. [32].

5. Summary and prospects

To summarize, measurements under high magnetic fields are important for understanding the variety of fascinating behaviors of heavy fermion systems. Measurements at high magnetic fields and low temperatures are important for experimentally probing the band structure, which provides a vital basis for understanding the physical properties. Tuning heavy fermion systems with field can show a marked difference to other tuning parameters, which can lead to different types of quantum critical behaviors. Nevertheless there are still many puzzling aspects associated with field induced quantum criticality and the interplay between magnetic order and the Kondo interaction when a field is applied. It is particularly important to understand systems exhibiting multiple types of QCP when tuned with different parameters, and the extent to which these QCPs can be universally classified will be the subject of future studies. Furthermore, for many recent topics of interest in

heavy fermion systems such as the role of topology or geometric frustration, measurements in magnetic fields have proved important for unveiling many of the novel properties.

High magnetic fields are also vital for directly probing the Fermi surface, which is a key method for classifying the different types of quantum critical points. Additional work is also required in this area to determine whether quantum phase transitions can be universally classified, and what happens to the quasiparticles upon approaching the different types of quantum critical points. A major experimental challenge in this regard is the need to measure the physical properties with a wide range of experimental tools both at very low temperatures and high magnetic fields, and the rapid development of measurements in high fields has provided a wealth of new information in recent years. Meanwhile Fermi surface probes in high magnetic fields are also important for probing topological materials. While topological materials have been well studied in weakly correlated systems, there are fewer examples of correlated topological materials. In particular, topological heavy fermion systems where the electronic bands are strongly renormalized by the Kondo interaction can allow for the interplay between topology and correlations to be examined.

Although high fields have been important for determining the superconducting order parameter, the novel superconducting states of heavy fermion superconductors can also show a number of unusual field-induced behaviors which still need to be explored. In particular, the so-called Q-phase of $CeCoIn_5$ shows an especially unusual and intriguing interplay of superconductivity and magnetism. In addition, the superconducting states of other heavy fermion superconductors are often not well characterized, which often require measurements both under pressure and very low temperatures to understand the superconducting properties.

Acknowledgment

We would like to thank E. D. Bauer, D. Graf, M. Jaime, Y. Kohama, H. Lee, K. Miyake, T. Park, Q. Si, J. Singleton, F. Steglich, J. D. Thompson, and J. X. Zhu for fruitful discussions.

References

[1] Hewson A C 1993 *The Kondo Problem to Heavy Fermions* (Cambridge: Cambridge University Press)
[2] Coleman P 2007 *Handbook of Magnetism and Advanced Magnetic Materials* Vol. **1** (New York: Wiley)
[3] Ruderman M A and Kittel C 1954 *Phys. Rev.* **96** 99
[4] Kasuya T 1956 *Prog. Theor. Phys.* **16** 45
[5] Yosida K 1957 *Phys. Rev.* **106** 893
[6] Doniach S 1977 *Phys. B+ C* **91** 231
[7] Chen Y, Weng Z, Smidman M, Lu X and Yuan H Q 2016 *Chin. Phys. B* **25** 077401
[8] Weng Z F, Smidman M, Jiao L, Lu Xin and Yuan H Q 2016 *Rep. Prog. Phys.* **79** 094503
[9] Gegenwart P, Custers J, Geibel C, Neumaier K, Tayama T, Tenya K, Trovarelli O and Steglich F 2002 *Phys. Rev. Lett.* **89** 056402
[10] Custers J, Gegenwart P, Wilhelm H, Neumaier K, Tokiwa Y, Trovarelli O, Geibel C, Steglich F, Pepin C and Coleman P 2003 *Nature* **424** 524
[11] Si Q, Rabello S, Ingersent K and Smith J L 2001 *Nature* **413** 804
[12] Coleman P, Pepin C, Si Q and Ramazashvili R 2001 *J. Phys.: Condens. Matter* **13** R723
[13] Si Q and Steglich F 2010 *Science* **329** 1161
[14] Dzero M, Sun K, Galitski V and Coleman P 2010 *Phys. Rev. Lett.* **104** 106408
[15] Li G, Xiang Z, Yu F, Asaba, T, Lawson B, Cai P, Tinsman C, Berkly A, Wolgast S, Eo Y S, Kim Dae-Jeong, Kurdak C, Allen J W, Sun X, Chen X H, Wang Y Y, Fisk Z and Li L 2014 *Science* **346** 1208
[16] Tan B S, Hsu Y T, Zeng B, Hatnean M C, Harrison N, Zhu Z, Hartstein M, Kiourlappou M, Srivastava A, Johannes M D, Murphy T P, Park J H, Balicas L, Lonzarich G G, Balakrishnan G and Sebastian S E 2015 *Science* **349** 287
[17] Hartstein M, Toews W H, Hsu Y T, Zeng B, Chen X, Hatnean M C, Zhang Q R, Nakamura S, Padgett A S, Rodway-Gant G, Berk J, Kingston M K, Zhang G H, Chan M K, Yamashita S, Sakakibara T, Takano Y, Park J H, Balicas L, Harrison N, Shitsevalova N, Balakrishnan G, Lonzarich G, Hill R W, Sutherland M and Sebastian S E 2017 *Nat. Phys.* **14** 166
[18] Luo Y, Chen H, Dai J, Xu Z A and Thompson J D 2015 *Phys. Rev. B* **91** 075130
[19] Chen F, Shang C, Jin Z, Zhao D, Wu Y P, Xiang Z J, Xia Z C, Wang A F, Luo X G, Wu T and Chen X H 2015 *Phys. Rev. B* **91** 205133
[20] Nakajima Y, Syers P, Wang X, Wang R and Paglione J 2016 *Nat. Phys.* **12** 213
[21] Xu Y, Cui S, Dong J K, Zhao D, Wu T, Chen X H, Sun K, Yao H and Li S Y 2016 *Phys. Rev. Lett.* **116** 246403
[22] Armitage N P, Mele E J and Vishwanath A 2018 *Rev. Mod. Phys.* **90** 015001
[23] Hasan M Z, Xu S Y, Belopolski I and Huang S M 2017 *Ann. Rev. Cond. Mat. Phys.* **8** 289
[24] Mikitik G P and Sharlai Y V 1999 *Phys. Rev. Lett.* **82** 2147
[25] Luk'yanchuk I A and Kopelevich Y 2004 *Phys. Rev. Lett.* **93** 166402
[26] Murakawa H, Bahramy M S, Tokunaga M, Kohama Y, Bell C, Kaneko Y, Nagaosa N, Hwang H Y and Tokura Y 2013 *Science* **342** 1490
[27] Wu F, Guo C Y, Smidman M, Zhang J L, Chen Y, Singleton J and Yuan H Q 2018 arXiv: 1807.03070
[28] Nielsen H and Ninomiya M 1983 *Phys. Lett. B* **130** 389
[29] Son D T and Spivak B Z 2013 *Phys. Rev. B* **88** 104412
[30] Huang X, Zhao L X, Long Y J, Wang P P, Chen D, Yang Z H, Liang H, Xue M Q, Weng H M, Fang Z, Dai X and Chen G F 2015 *Phys. Rev. X* **5** 031023
[31] Guo C Y, Cao C, Smidman M, Wu F, Zhang Y J, Steglich F, Zhang F C and Yuan H Q 2017 *Npj Quantum Mater.* **2** 39
[32] Guo C Y, Wu F, Wu Z Z, Smidman M, Cao C, Bostwick A, Jozwiak C, Rotenberg E, Liu Y, Steglich F and Yuan H Q 2018 *Nat. Commun.* **9** 4622
[33] Yuan H Q, Grosche F M, Deppe M, Geibel C, Sparn G and Steglich F 2003 *Science* **302** 2104
[34] Yuan H Q, Grosche F M, Deppe M, Sparn G, Geibel C and Steglich F 2006 *Phys. Rev. Lett.* **96** 047008
[35] Holmes A T, Jaccard D and Miyake K 2004 *Phys. Rev. B* **69** 024508
[36] Lawrence J M and Shapiro S M 1980 *Phys. Rev. B* **22** 4379
[37] Mathur N D, Grosche F M, Julian S R, Walker I R, Freye D M, Haselwimmer R K W and Lonzarich G G 1998 *Nature* **394** 39
[38] Hegger H, Petrovic C, Moshopoulou E G, Hundley M F, Sarrao J L, Fisk Z and Thompson J D 2000 *Phys. Rev. Lett.* **84** 4986
[39] Petrovic C, Pagliuso P G, Hundley M F, Movshovich R, Sarrao J L, Thompson J D, Fisk Z and Monthoux P 2001 *J. Phys.: Condens. Matter* **13** L337
[40] Petrovic C, Movshovich R, Jaime M, Pagliuso P G, Hundley M F, Sarrao J L, Fisk Z and Thompson J D 2001 *Europhys. Lett.* **53** 354
[41] Knebel G, Aoki D, Braithwaite D, Salce B and Flouquet J 2006 *Phys. Rev. B* **74** 020501
[42] Park T, Ronning F, Yuan H Q, Salamon M B, Movshovich R, Sarrao J L and Thompson J D 2006 *Nature* **440** 65
[43] Chen G, Ohara S, Hedo M, Uwatoko Y, Saito K, Sorai M and Sakamoto I 2002 *J. Phys. Soc. Jpn.* **71** 2836

[44] Nicklas M, Sidorov V A, Borges H A, Pagliuso P G, Petrovic C, Fisk Z, Sarrao J L and Thompson J D 2003 *Phys. Rev. B* **67** 020506

[45] Kaczorowski D, Pikul A P, Gnida D and Tran V H 2009 *Phys. Rev. Lett.* **103** 027003

[46] Shishido H, Settai R, Aoki D, Ikeda S, Nakawaki H, Nakamura N, Iizuka T, Inada Y, Sugiyama K, Takeuchi T, Kindo K, Kobayashi T C, Haga Y, Harima H, Aoki Y, Namiki T, Sato H and Yoshichika O 2002 *J. Phys. Soc. Jpn.* **71** 162

[47] Harrison N, Alver U, Goodrich R G, Vekhter I, Sarrao J L, Pagliuso P G, Moreno N O, Balicas L, Fisk Z, Hall D, Macaluso Robin T and Chan J Y 2004 *Phys. Rev. Lett.* **93** 186405

[48] Jiao L, Chen Y, Kohama Y, Graf D, Bauer E D, Singleton J, Zhu J X, Weng Z F, Pang G M, Shang T, Zhang J L, Lee H O, Park T, Jaime M, Thompson J D, Steglich F, Si Q M and Yuan H Q 2015 *Proc. Natl Acad. Sci. USA* **112** 673

[49] Shishido H, Settai R, Harima H and Ōnuki Y 2005 *J. Phys. Soc. Jpn.* **74** 1103

[50] Hall D, Palm E C, Murphy T P, Tozer S W, Fisk Z, Alver U, Goodrich R G, Sarrao J L, Pagliuso P G and Ebihara T 2001 *Phys. Rev. B* **64** 212508

[51] Jiao L, Weng Z F, Smidman M, Graf D, Singleton J, Bauer E D, Thompson J D and Yuan H Q 2017 *Philos. Mag.* **97** 3446

[52] Ronning F, Helm T, Shirer K R, Bachmann M D, Balicas L, Chan M K, Ramshaw B J, McDonald R D, Balakirev F F, Jaime M, Bauer E D and Moll P J W 2017 *Nature* **548** 313

[53] Dong J K, Zhang H, Qiu X, Pan B Y, Dai Y F, Guan T Y, Zhou S Y, Gnida D, Kaczorowski D and Li S Y 2011 *Phys. Rev. X* **1** 011010

[54] Paglione J, Tanatar M A, Hawthorn D G, Boaknin E, Hill R W, Ronning F, Sutherl M, Taillefer L, Petrovic C and Canfield P C 2003 *Phys. Rev. Lett.* **91** 246405

[55] Bianchi A, Movshovich R, Vekhter I, Pagliuso P G and Sarrao J L 2003 *Phys. Rev. Lett.* **91** 257001

[56] Bramwell S T and Gingras M J P 2001 *Science* **294** 1495

[57] Kim M S and Aronson M C 2013 *Phys. Rev. Lett.* **110** 017201

[58] Coleman P and Nevidomskyy A H 2010 *J. Low Temp. Phys.* **161** 182

[59] Si Q 2006 *Physica B* **378–380** 23

[60] Custers J, Gegenwart P, Geibel C, Steglich F, Coleman P and Paschen S 2010 *Phys. Rev. Lett.* **104** 186402

[61] Hulliger F 1993 *J. Alloys Compd.* **196** 225

[62] Dönni A, Ehlers G, Maletta H, Dönni, A, Ehlers G, Maletta H, Fischer P, Kitazawa H and Zolliker M 1996 *J. Phys. Condens. Matter* **8** 11213

[63] Oyamada A, Maegawa S, Nishiyama M, Oyamada A, Maegawa S, Nishiyama M, Kitazawa H and Isikawa Y 2008 *Phys. Rev. B* **77** 064432

[64] Lucas S, Grube K, Huang C L, Sakai A, Wunderlich S, Green E L, Wosnitza J, Fritsch V, Gegenwart P, Stockert O and Löhneysen H V 2017 *Phys. Rev. Lett.* **118** 107204

[65] Zhao H C, Zhang J H, Hu S L, Zhao H, Zhang J, Hu S, Isikawa Y, Luo J, Steglich F and Sun P 2016 *Phys. Rev. B* **94** 235131

[66] Movshovich R, Jaime M, Thompson J D, Petrovic C, Fisk Z, Pagliuso P G and Sarrao J L 2001 *Phys. Rev. Lett.* **86** 5152

[67] Chia E E M, Van Harlingen D J, Salamon M B, Yanoff B D, Bonalde I and Sarrao J L 2003 *Phys. Rev. B* **67** 014527

[68] Vandervelde, D, Yuan H Q, Ōnuki Y and Salamon M B 2009 *Phys. Rev. B* **79** 212505

[69] Lu X, Lee H, Park T, Ronning F, Bauer E D and Thompson J D 2012 *Phys. Rev. Lett.* **108** 027001

[70] Vorontsov A B and Vekhter I 2007 *Phys. Rev. B* **75** 224501

[71] An K, Sakakibara T, Settai R, Onuki Y, Hiragi M, Ichioka M and Machida K 2010 *Phys. Rev. Lett.* **104** 037002

[72] Izawa K, Yamaguchi H, Matsuda Y, Shishido H, Settai R and Onuki Y 2001 *Phys. Rev. Lett.* **87** 057002

[73] Kasahara Y, Iwasawa T, Shimizu Y, Shishido H, Shibauchi T, Vekhter I and Matsuda Y 2008 *Phys. Rev. Lett.* **100** 207003

[74] Fulde P and Ferrell R A 1964 *Phys. Rev.* **135** A550

[75] Larkin A I and Sov Y N 1965 *Phys. JETP* **20** 762

[76] Bianchi A, Movshovich R, Oeschler N, Gegenwart P, Steglich F, Thompson J D, Pagliuso P G and Sarrao J L 2002 *Phys. Rev. Lett.* **89** 137002

[77] Bianchi A, Movshovich R, Capan C, Pagliuso P G and Sarrao J L 2003 *Phys. Rev. Lett.* **91** 187004

[78] Radovan H A, Fortune N A, Murphy T P, Hannahs S T, Palm E C, Tozer S W and Hall D 2003 *Nature* **425** 51

[79] Kakuyanagi K, Saitoh M, Kumagai K, Takashima S, Nohara M, Takagi H and Matsuda Y 2005 *Phys. Rev. Lett.* **94** 047602

[80] Mitrović V F, Horvatić M, Berthier C, Knebel G, Lapertot G and Flouquet J 2006 *Phys. Rev. Lett.* **97** 117002

[81] Young B L, Urbano R R, Curro N J, Thompson J D, Sarrao J L, Vorontsov A B and Graf M J 2007 *Phys. Rev. Lett.* **98** 036402

[82] Kenzelmann M, Strässle T, Niedermayer C, Sigrist M, Padmanabhan B, Bianchi A D, Movshovich R, Bauer E D, Sarrao J L and Thompson J D 2008 *Science* **321** 1652

[83] Kenzelmann M, Gerber S, Egetenmeyer N, Gavilano J L, Strässle T, Bianchi A D, Ressouche E, Movshovich R, Bauer E D, Sarrao J L and Thompson J D 2010 *Phys. Rev. Lett.* **104** 127001

[84] Gerber S, Bartkowiak M, Gavilano J L, Ressouche E, Egetenmeyer N, Niedermayer C, Bianchi A D, Movshovich R, Bauer E D, Thompson J D and Kenzelmann M 2014 *Nat. Phys.* **10** 126

[85] Agterberg D F, Sigrist M and Tsunetsugu H 2009 *Phys. Rev. Lett.* **102** 207004

[86] Aperis A, Varelogiannis G and Littlewood P B 2010 *Phys. Rev. Lett.* **104** 216403

[87] Kim D Y, Lin S Z, Weickert F, Kenzelmann M, Bauer E D, Ronning F, Thompson J D and Movshovich R 2016 *Phys. Rev. X* **6** 041059

[88] Riseborough P S 2000 *Adv. Phys.* **49** 257

[89] Menth A, Buehler E and Geballe T H 1969 *Phys. Rev. Lett.* **22** 295

[90] Allen J W, Batlogg B and Wachter P 1979 *Phys. Rev. B* **20** 4807

[91] Wolgast S, Kurdak Ç, Sun K, Allen J W, Kim D J and Fisk Z 2013 *Phys. Rev. B* **88** 180405

[92] Kim D J, Thomas S, Grant T, Botimer J, Fisk Z and Xia J 2013 *Sci. Rep.* **3** 3150

[93] Kim D J, Xia J and Fisk Z 2014 *Nat. Mater.* **13** 466

[94] Erten O, Ghaemi P and Coleman P 2016 *Phys. Rev. Lett.* **116** 046403

[95] Knolle J and Cooper N R 2017 *Phys. Rev. Lett.* **118** 096604

[96] Erten O, Chang P Y, Coleman P and Tsvelik A M 2017 *Phys. Rev. Lett.* **119** 057603

[97] Xu S Y, Belopolski I, Alidoust N, Neupane M, Bian G, Zhang C, Sankar R, Chang G Q, Yuan Z J, Lee C C, Huang S M, Zheng H, Ma J, Sanchez D S, Wang B K, Bansil A, Chou F C, Shibayev P P, Lin Hsin, Jia S and Hasan M Z 2015 *Science* **349** 613

[98] Lv B Q, Xu N, Weng H M, Ma J Z, Richard P, Huang X C, Zhao L X, Chen G F, Matt C E, Bisti F, Strocov V N, Mesot J, Fang Z, Dai X, Shi M and Ding H 2015 *Nat. Phys.* **11** 724

[99] Yang L X, Liu Z K, Sun Y, Peng H, Yang H F, Zhang T, Zhou B, Zhang Y, Guo Y F, Prabhakaran Rahn M, Hussain Z, Mo S K, Felser C, Yan B and Chen Y L 2015 *Nat. Phys.* **11** 728

[100] Lv B Q, Weng H M, Fu B B, Wang X P, Miao H, Ma J, Richard P, Huang X C, Zhao L X, Chen G F, Fang Z, Dai X, Qian T and Ding H 2015 *Phys. Rev. X* **5** 031013

[101] Tafti F F, Gibson Q D, Kushwaha S K, Haldolaarachchige N and Cava R J 2016 *Nat. Phys.* **12** 272

[102] Niu X H, Xu D F, Bai Y H, Song Q, Shen X P, Xie B P, Sun Z, Huang Y B, Peets D C and Feng D L 2016 *Phys. Rev. B* **94** 165163

[103] Zeng L K, Lou R, Wu D S, Xu Q N, Guo P J, Kong L Y, Liu T, Lu L, Huang Y B, Fang C, Sun S S, Wang Q, Wang L, Shi Y G, Weng H M, Lei H C, Liu K, Wang S C, Qian T, Luo J L and Ding H 2016 *Phys. Rev. Lett.* **117** 127204

[104] Wu F, Guo C Y, Smidman M, Zhang J L and Yuan H Q 2017 *Phys. Rev. B* **96** 125122

[105] Li P, Wu Z, Wu F, Cao C, Guo C, Wu Y, Liu Y, Sun Z, Cheng C M, Lin D S, Steglich F, Yuan H Q, Chiang T C and Yang L 2018 *Phys. Rev. B* **98** 085103

[106] Duan X, Wu F, Chen J, Zhang P, Liu Y and Yuan H C 2018 arXiv: 1802.04554

[107] Fisk, Z, Canfield P C, Beyermann W P, Thompson J D, Hundley M F, Ott H R, Felder E, Maple M B, Lopez M A, de la Torre, Visani P and Seaman C L 1991 *Phys. Rev. Lett.* **67** 3310